**Article ID:** 1003 - 6326(2004) 02 - 0284 - 07

# Effect of alloying elements on mechanical properties in Cu-15% Cr in situ composites

H. G. Suzuki<sup>1,2</sup>, J. Ma<sup>2</sup>, K. Mihara<sup>3</sup>, S. Sakai<sup>3</sup>, S. Sun<sup>4</sup>

- (1. Japan Society for Promotion of Science, 4-1-8, Hon-machi, Kawaguchi, 332-0012, Japan;
- 2. Department of Materials Science and Engineering, Tsinghua University, Beijing 100084, China;
  - 3. Furukawa Electric CO, LTD, Nikko, 321-0014, Japan;
  - 4. National Institute for Materials Science, Tsukuba, 305-0047, Japan)

**Abstract:** The effects of alloying elements on the mechanical properties as well as electrical conductivity in Cur 15% Cr (mass fraction) irrisitu composites were systematically studied and high strength and high electrical conductive Cu base irrisitu composites have been developed. The best combination is the addition of 0.1% to 0.2% Zr, Ti, or Sn in Cur 15% Cr irrisitu composite, thermomechanical treatment to refine the microstructure and optimizing the precipitation of second phase. The strength is controlled by high density of dislocations in the Cu matrix, the lamellar spacing of the second phase, and the fine Cr precipitates. The aging treatment to reduce solute atoms has a beneficial effect on the increase of electrical conductivity. The addition of Zr, or Ti of about 0.15% to 0.2% promotes the precipitation of Cr particles.

**Key words:** Cu alloy; in situ composite; high strength; conductivity; thermomechanical treatment; aging; precipitation

CLC number: TG 146.2 Document code: A

### 1 INTRODUCTION

The demand for high strength and high electrical conductive materials has become potent for this sustainable society. We have already developed Cu-15% Cr (15Cr) irrsitu composites having the tensile strength level of 850 MPa and electrical conductivity (EC) of 75% IACS by optimizing thermomechanical treatment<sup>[1-4]</sup>. High strength is attained by high density of dislocations in the Cu matrix and narrowing the interlamellar spacing of the Cr second phase through the cold drawing. The additional increase of the strength and high EC was obtained by the precipitation of fine Cr in the Cu matrix on aging treatment after cold drawing.

In this paper, the effect of microalloying such as Zr, Ti, Sn, Fe, and Si is described.

## 2 EXPERIMENTAL

The alloys were produced by melting the mixture of Cu, Cr, Sn, Ni, Si with purity of 99.99% and Cur 50% Zr or Cur 30% Ti master alloys using high frequency vacuum induction melting furnace. The nominal compositions of these alloys are Cur 15% Cr-0. 15% Zr(15CZ)<sup>[6,7]</sup>, Cur 15% Cr-0. 2% Ti(15CT)<sup>[8]</sup>, Cur 15% Cr-0. 1% Sn(15C1S)<sup>[9]</sup>, Cur 15% Cr-0. 5% Fe(15C5F)<sup>[9]</sup> and Cur 15% Cr-0. 5% Si<sup>[10]</sup>.

The manufacturing process is schematically

shown in Fig. 1. All the ingots were hot forged at 1 173 K to break the cast structure and produce slabs of 23 mm in thickness, and then solution treated at 1 273 K for 1 h, followed by water quenching. Cold drawing was performed using cassette roller dice (Yoshida Kinen Co.). In order to get almost the same size of final wire specimens (0.69 mm to 1 mm in diameter), the starting materials were sliced into the cross sectional area from 1. 7 mm<sup>2</sup> to 402 mm<sup>2</sup>. Thus, the cold drawing strain has changed from  $\eta = 0$ to 6.9. Here,  $\eta = \ln(A_0/A)$ ,  $A_0$  is the initial cross sectional area of the specimen, and A is the final one. After cold drawing, wire specimens were subjected to the aging treatment in the range from 623 K to 1 023 K for 1 h, which was named as STCA specimens. STC specimens were just solution treated and cold rolled and STA means aging just after solution treatment.

Microhardness was measured for both Cu and Cr phases in the as solution treated specimens at the load of 49 N and the present results are average of 10 testing values. Microstructural examination was done by optical microscopy, SEM (JSM-6100) and TEM (JEM-2000FX) attached by EDX analyzer. The thickness of the deformed Cr phase and the spacing between the Cr phase (= d, defined here as an interlamellar spacing) after cold drawing were measured on the longitudinal section of as drawn in situ com-

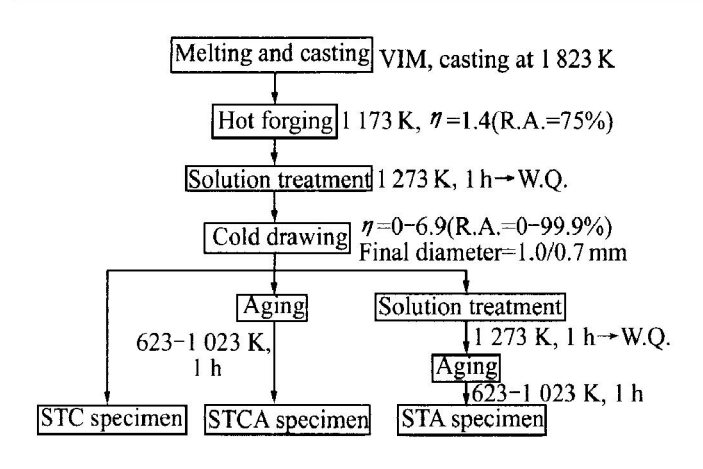


Fig. 1 Schematic presentation of processing flow of Cu-Cr in-situ composites

posites, and averaged among 30 measurements.

Tensile test was performed by Instrom-type DDS-10T (Shimadzu) testing machine. The size of the specimen is 100 mm in length and 0.7 to 1 mm in diameter. Cross head speed was 2 mm/min.  $\sigma_{0.2}$  means 0.2% proof stress and  $\sigma_{b}$  is the tensile strength.

EC of wire specimens was measured by four point terminal method in a thermostatic bath at 293 K. It was then calculated as an average of two measurements with the polarity reversed on the terminals 200 mm apart. The unit, % IACS, is per cent of international annealed copper standard.

### 3 RESULTS AND DISCUSSION

### 3. 1 Effect of Sn

Dendritic Cr deforms along rolling direction and fine lamellar structure is formed after heavy deformation such as  $\eta = 6.37$ , resulting in the in situ composite. Fig. 2 shows both the Cr lamellar spacing (d) and thickness of the Cr lamellar (t) against cold drawing strain. Maximum drawing strain was  $\eta = 6$ . 37 and d was 0.8  $\mu$ m, where fracture occurred by shearing the Cr lamellar. The dependence of t and don I is derived by the least square fitting method as follows:  $t = 3.25 \exp(-0.29 \, \text{I})$ ,  $d = 12.04 \exp(-0.29 \, \text{I})$ 0. 45  $\eta$ ) for 15C5S and  $t = 7.58 \cdot \exp(-0.42 \eta)$ , d = 7.  $18\exp(-0.31 \, \text{\refthat{N}})$  for 15C1S. The square shape data in this figure is for 15Cr, which indicates the lamellar spacing of two Sn doped alloys is coarser than that of 15Cr. One reason for this is due to the initial coarse dendrite structure of Sn doped alloys. The tensile strength increases with the drawing strain, and shows more clearly the beneficial effect of Sn addition. The increase of the strength is evident even in 15C1S, low Sn content. The maximum strength attained is 1 000 MPa in 15C1S. Both  $\sigma_{0,2}$  and  $\sigma_{b}$  were plotted as a function of lamellar spacing d (Fig. 3), which shows a linear relationship between strength

and  $d^{-1/2}$  suggesting Hall-Petch like relationship exists in this cold rolled alloys as was already discussed<sup>[1, 5, 8]</sup>. Fig. 4 shows the hardness change with aging temperature, where open circle and open square data are STA treated ones and solid circle and solid square data are from the STCA (cold rolled and aged). Both results of STA and STCA clearly show that there exists the secondary hardening due to the precipitation and peak temperature lies at around 750 K. On the other hand, in the STCA process, peak hardness is shifted to lower temperature at around 700 K and peak hardness reached Hv 200 due to the acceleration of precipitation of Cr on the defects introduced by cold drawing. It is evident from these data that the addition of Sn to 15Cr is effective to increase the hardness.

The data for EC against aging temperature is shown in Fig. 5. It is noted that EC recovers from

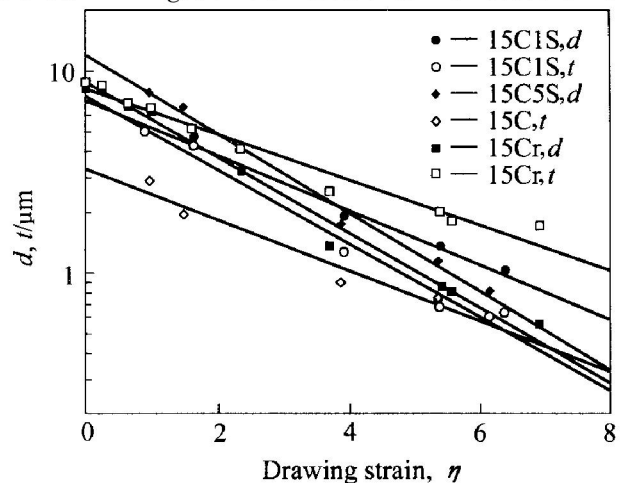


**Fig. 2** Effect of drawing strain on spacing(d) and thickness(t) of Cr phase in Cur 15% Cr-0. 1% Sn (15C1S), Cur 15% Cr-0. 5% Sn(15C5S) and Cur 15% Cr(15Cr)

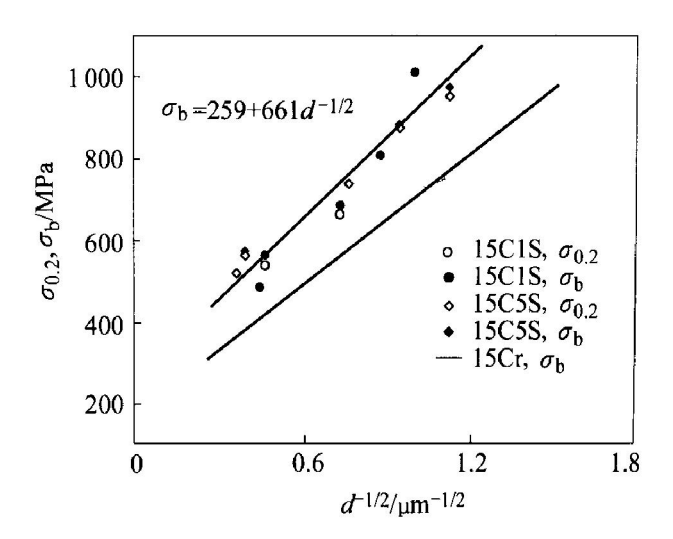


Fig. 3 Relation between  $\sigma_{0.2}$ , tensile strength and spacing of Cr, d, in cold drawn 15C1S, 15C5S and 15Cr

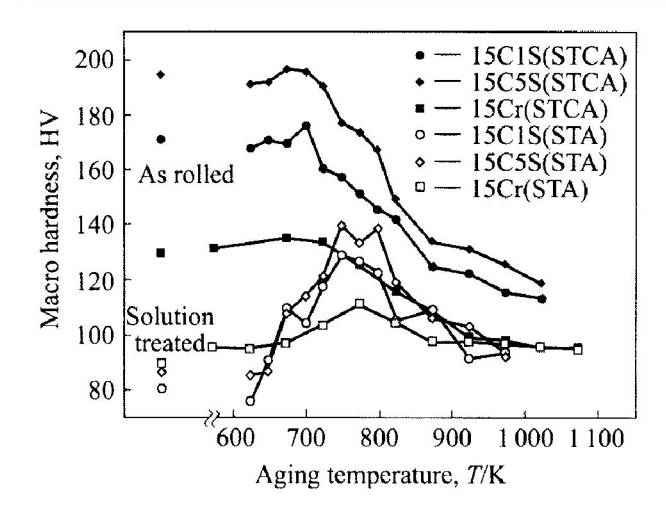


Fig. 4 Effect of aging temperature on macrohardness of STCA specimens in 15C1S, 15C5S and 15Cr (Drawing strain is  $\eta = 5.3$  for 15C1S, 15C5S and  $\eta = 5$  for 15Cr)

the beginning of the aging treatment and increases with the irrement of aging temperature, reaching maximum between 800 K and 900 K and then goes down again. This behavior corresponds to the precipitation and re-solutioning of Cr precipitates in the Cu matrix and quite similar characteristics to those of already reported ones<sup>[3-5]</sup>. It is noted that aging temperature giving the EC maximum is the overaged region, where the strength goes down.

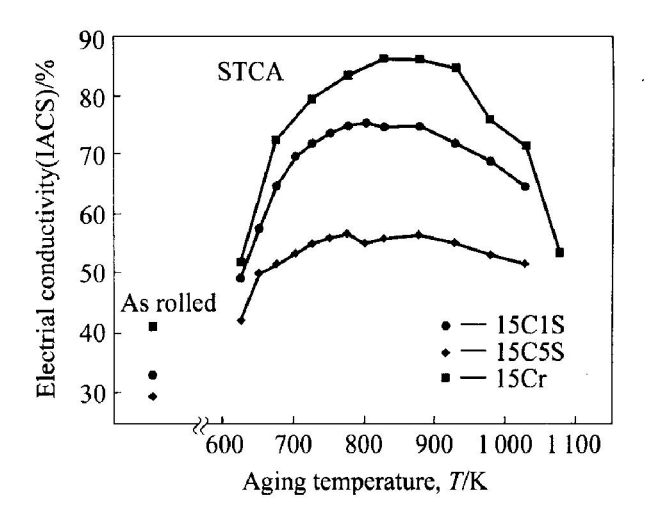


Fig. 5 Effect of aging temperature on electrical conductivity of STCA specimens in 15C1S, 15C5S and 15Cr (Drawing strain is  $\eta$ = 5.3 for 15C1S, 15C5S and  $\eta$ = 5 for 15Cr)

In the microstructure at the aging temperature of 698 K, which corresponds to the peak hardness, high density of dislocations, banded structure and fine precipitates on the dislocations as well as in the matrix were observed as shown in Fig. 6. These precipitates were determined as Cr by EDS in situ analysis and there was no signal corresponding to Sn.

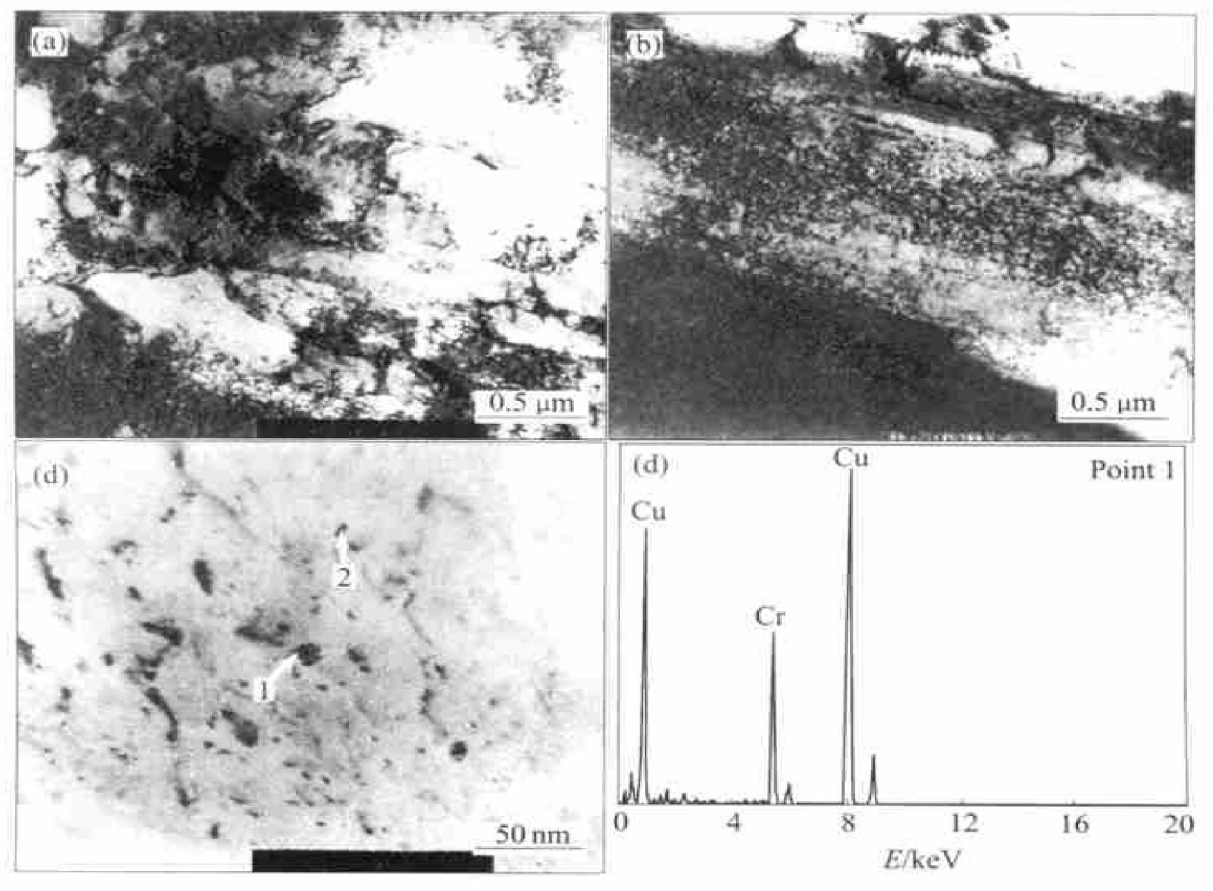


Fig. 6 TEM bright field images and EDS spectrum of STCA specimen in 15C1S alloy (  $\eta$ = 5.3 and aged at 698 K for 1 h)

(a) —High density of dislocation; (b) —Banded structure; (c) —Fine precipitates; (d) —EDS spectrum

### 3. 2 Effect of microalloying of either Zr or Ti

The tensile strength of Zr(15CZ) and Ti(15CT) added alloys in the cold rolled stage is shown in Fig. 7 together with other alloys. Zr added alloy shows about 200 MPa higher value than that of base 15Cr alloy with the same d spacing. This high strength is due to the following factors: high density of dislocations in the banded structure of the Cu matrix and refinement of the Cr lamellar spacing by cold drawing. The analysis of TEM microstructure has clarified these facts. Alloying element such as Zr or Ti may suppress the dynamic recrystallization and accumulate the dislocations introduced by cold drawing. The alloying of either Zr or Ti is more effective on the aging treatment to increase the mechanical as well as electrical properties. Cold drawing before the aging treatment is useful to increase both the strength and EC. The tensile strength of 1 150 MPa and EC of 71% I-ACS were attained by aging at 723 K for 1 h after cold drawing for  $\P$ = 6.9.

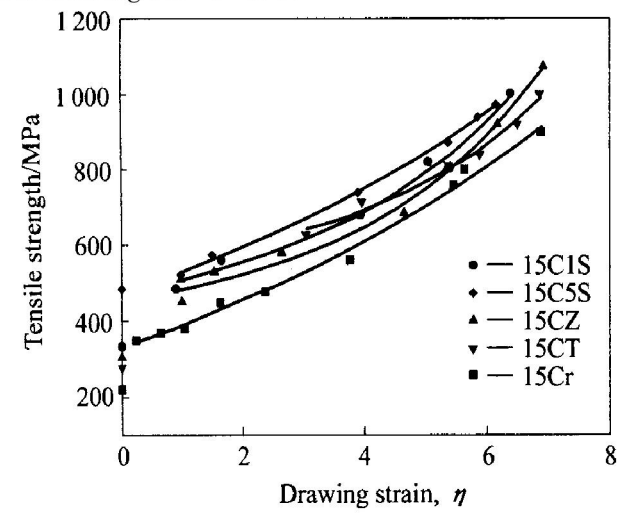


Fig. 7 Relationship between tensile strength and drawing strain in Cur15Cr(15Cr), Cur15Cr-0.15Zr (15CZ), Cur15Cr-0.2Ti(15CT), Cur15Cr-0.1Sn(15C1S) and Cur15Cr-0.5Sn(15C5S) alloys

# 3.3 Effects of alloying elements on microstructure and microhardness

The SEM backscattered electron images (BEI) of the solution treated Cur 15r-X alloys show that the Cr phase in all examined alloys is granular in shape. During the cast and the solution treatment at 1 273 K for 1 h, the partitioning of alloying elements in the Cu matrix and in the Cr second phase occurs depending on their chemical potentials to each phase. The chemical compositions of these elements in the Cu and Cr phases are tabulated in Table 1. Both Zr and Ti do segregate into the Cu matrix while both Si and Fe concentrate in the Cr phase, and Sn dissolves in both phases. These partitionings will give an influence on

the hardness of each phase by the solid solution hardening as seen in Table 2. Both Si and Fe strengthen the Cr phase significantly through solid solution hardening, whereas either Sn, Zr or Ti enhances very little.

**Table 1** Content of alloying elements in Cu matrix and Cr phases (mass fraction, %)

Elements and content in Cur 15Cr based alloys	Content of alloying element in Cu phase	Content of alloying element in Cr phase
0. 1Sn	0. 05	0. 31
0. 15Zr	0. 18	0.00
0. 2T i	0. 22	0.08
0. 2Fe	0.06	0.99
0.5Fe	0. 15	2. 46
0.5Si	0. 02	2. 36

**Table 2** Effect of alloying elements on microhardness of Cu and Cr phases

Elements and content/%	Hv of Cu phase	Hv of Cr phase	Hardness ratio of Cu to Cr phase/ %
no alloying element	80	200	0.40
0. 1Sn	90	190	0.47
0. 15Zr	92	190	0.48
0. 2T i	95	190	0.50
0.2Fe	90	232	0.39
0.5Fe	88	225	0.39
0. 5Si	90	245	0.37

### 3. 4 Effect of alloying elements on cold drawability

Fig. 8 shows typical microstructure after heavy cold drawing ( $\eta = 6.2$ ). In this picture, the deformation of the Cr phase in 15Cr, 15CZ, and 15C1S alloys is uniform, while some large Cr phases still remain undeformed in Cu-15Cr-0. 5Si. The deformation of the Cr phase is characterized in terms of deformation strain of the Cr phase,  $\mathcal{E}_{Cr}$ , which is defined as the natural logarithmic form of the ratio of initial thickness of the Cr phase (under the solution treated condition) to the final thickness of it ( $\mathcal{E}_{Cr} = \ln(t_0/t_0)$ t)). The relation between  $\mathcal{E}_{Cr}$  and drawing strain,  $\mathcal{E}$ , in the 15Cr base alloys is shown in Fig. 9. The harder Cr phase is subjected to the deformation below that of 15Cr base alloy, whereas the more ductile Cu matrix undergoes larger deformation, locally. The deformation strain partitioning between the Cu and the Cr phases can be explained by the difference of hardness and modulus between the two phases. The alloying elements change the deformation strain partitioning between the Cu matrix and the Cr second phase

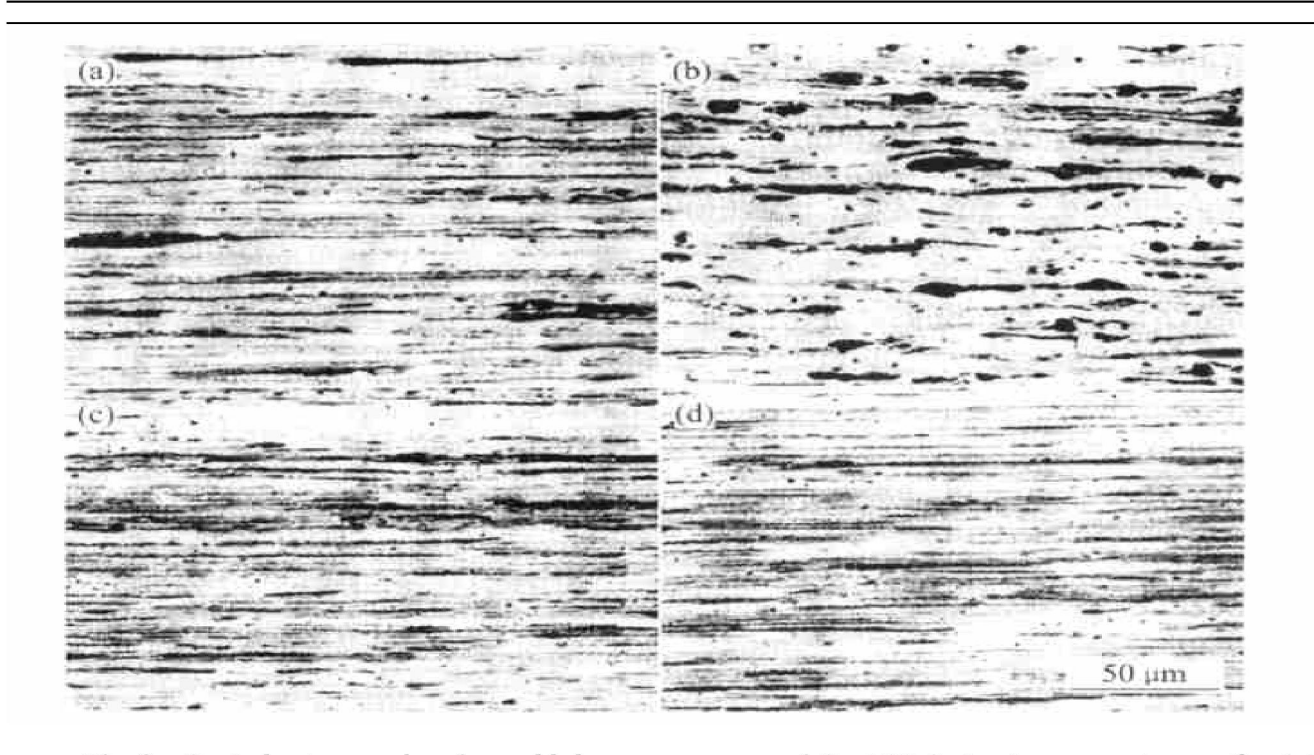


Fig. 8 Optical micrographs of as cold drawn structures of Cu-15% Cr in situ composites at ¬ = 6.2 (a) —Cu-15Cr; (b) —Cu-15Cr-0.5Si; (c) —Cu-15Cr-0.15Zr; (d) —Cu-15Cr-0.1Sn

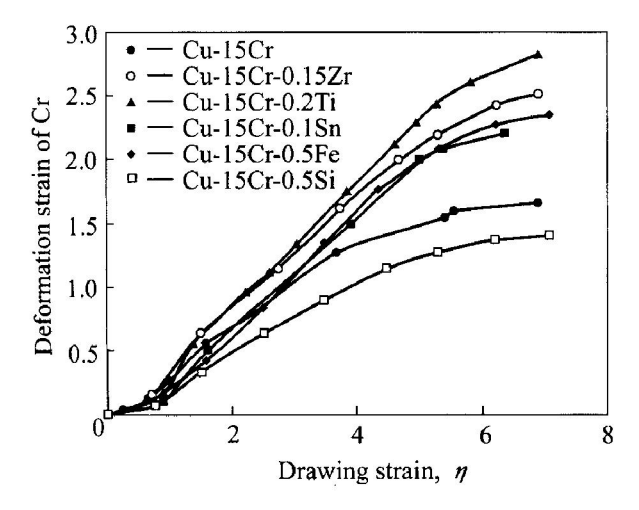


Fig. 9 Effect of alloying elements on deformation strain of Cr phase, plotted as a function of drawing strain, \(\eta\)

through the hardness change. The relation between the deformation strain of the Cr phase and drawing strain in the second stage can be written linearly as follows:  $\mathcal{E}_{Cr} = m \cdot \mathbb{I}$ . The m-value is the slope of  $\mathcal{E}_{Cr} - \mathbb{I}$  curves of the linear part in Fig. 9. The higher m-value means the larger deformation of the Cr occurs at the same drawing strain, hence the finer Cr fiber is obtained leading to higher strength. Using this parameter, the appreciation of cold draw ability is found to be possible. Fig. 10 shows the linear relationship between m-value and the hardness ratio of the Cu matrix to Cr phase,  $Hv_{Cr}/Hv_{Cr}$ . From this figure, it is shown that if m-value is higher than 0. 3 or hardness ratio,  $Hv_{Cu}/Hv_{Cr}$ , is bigger than 0. 45,

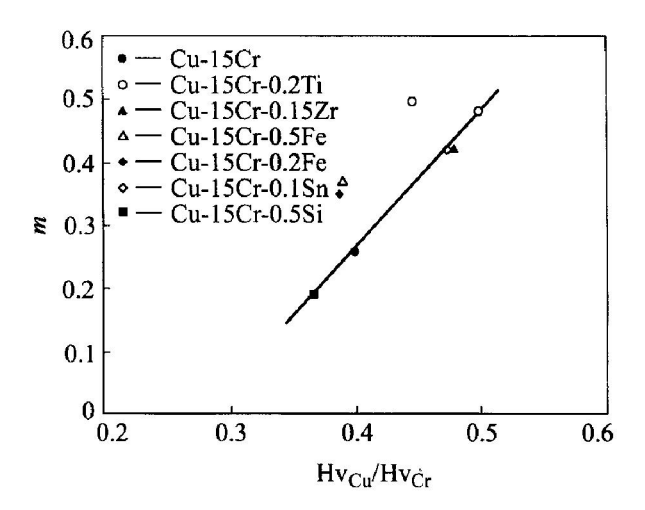


Fig. 10 Relation between m-value and hardness ratio,  $Hv_{Cu}/Hv_{C}$ 

workability is superior. 15CT and 15CZ alloys show a very good drawability, followed by fine lamellar spacing and high strength.

### 3. 5 Strengthening mechanism

As already shown in Figs. 3 and 7, the strength depends on the work hardening of the Cu matrix and the Cr second phase and interlamellar spacing of the Cr phase in the cold drawn stage. The tensile strength as well as  $\sigma_{0.2}$  follows Hall-Petch type equation. Alloying element such as Sn, Zr or Ti increases the flow stress level through high density of dislocations and banded structure in the Cu matrix.

Sun<sup>®</sup>, one of the present authors, described

the strengthening equation of the present Cu base insitu composites based on the rule of mixture and taking into account of the contribution of the strain hardening in two phases as follows:

$$\sigma = \sigma_{0} + kd^{-1/2}$$

$$\sigma_{0} = \Psi_{Cu} \{ \sigma_{0} (Cu) + A (Cu) \mathcal{E}^{u} (Cu) \} + \Psi_{Cr} \{ \sigma_{0} (Cr) + A (Cr) \mathcal{E}^{u} (Cr) \}$$
(1)

Here  $\sigma_0$ , k and A are the constants and  $\phi$  is the volume fraction. This equation describes the effect of work hardening of each phase and the effectiveness of the Cr fibers as barriers to the dislocation motion respectively.

Based on the result of Cu 15% Cr 0. 5% Si alloy, the contribution of each factor is calculated using equation (1) as in the followings. The strength of solution treated alloy without cold drawing is the contribution from  $(\Phi_{Cr} \circ (Cu)_0 + \Phi_{Cr} \circ (Cr)_0)$ , 289 MPa. The contribution of each strengthening mechanism a gainst drawing strain is plotted in Fig. 11. The work hardening of the Cu matrix increases abruptly in the initial stage of cold drawing. The contribution from work hardening and interlamellar spacing of the Cr second phase increases continuously with the drawing strain. It is clear that work hardening of the Cu matrix plays more important role in the strengthening at lower drawing strain, while work hardening of the Cr phase and interlamellar spacing of the Cr phase are the principal strengthening contributions to the Cur 15% Cr-0. 5% Si alloy at higher strain stage. Biselli et al<sup>[12]</sup> have reported the strengthening mechanism of similar heavily deformed Cu-Fe in-situ composites assuming second phase of Fe stays constant of 0.2% of elastic modulus. Fig. 12 shows the result of the comparison between the present result and the Biselli's prediction<sup>[11]</sup>, which shows higher strength at lower drawing strain.

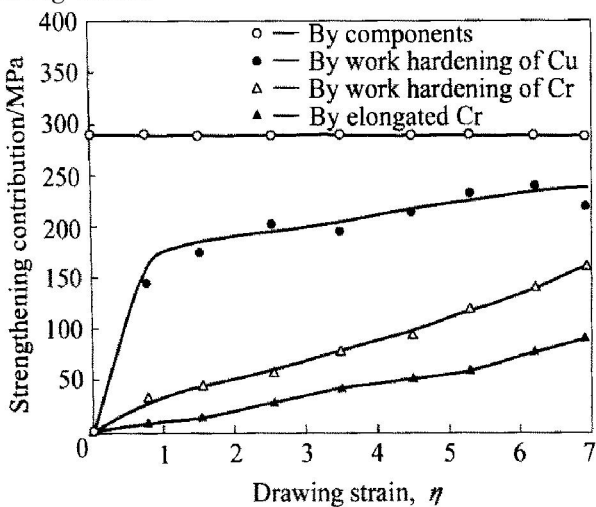


**Fig. 11** Contributions of strengthening mechanism in Cu-15% Cr-0. 5% Si alloy

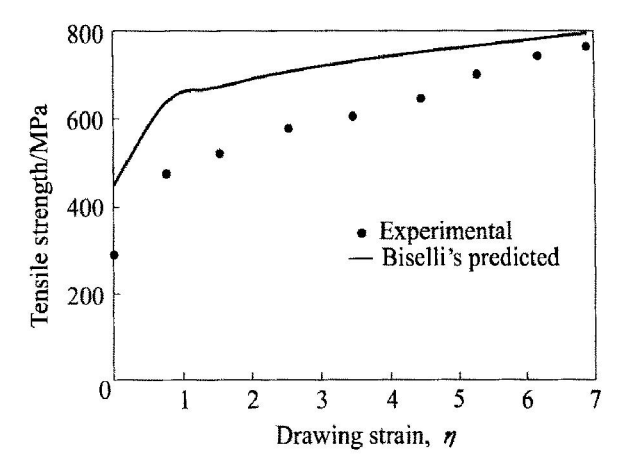


Fig. 12 Experimental data and Biselli's predicted tensile strength of Cu 15% Cr-0. 5% Si alloy

### 4 CONCLUSIONS

- 1) The addition of 0. 1% to 0. 2% of Zr, Ti or Sn in Cu 15% Cr in situ composites and optimizing the thermomechanical processing such as cold drawing and aging give the tensile strength of more than 1 000 MPa and electrical conductivity of more than 70% I-ACS.
- 2) The tensile strength is controlled by the work hardening of the Cu and the Cr phases due to the severe cold drawing, interlamellar spacing of the Cr phase and fine precipitates of Cr in the Cu matrix.
- 3) The strength of cold drawn composite is formulated by the following equation,

Here  $\sigma_0$ , k and A are the constants and  $\phi$  is the volume fraction. This equation describes the effect of work hardening of each phase and the effectiveness of the Cr fibers as barriers to the dislocation motion respectively.

4) The addition of Si or Fe increases the hardness of the Cr phase by solid solution hardening and makes the cold drawability of Cu-15% Cr in situ composites poor.

### Acknowledgements

The authors want to express their thanks to National Institute for Materials Science, Japan. This work was mainly done in this institute with the aid of NEDO. The authors would like to express the thanks to Furukawa Electric Co. LTD. for the financial support. The faculty members of Department of Materials Science and Engineering, Tsinghua University are greatly appreciated for their support of H. G. Suzuki, one of authors for staying as a visiting professor. Special thanks are to Dr. Wang Guang-long of the same University giving important advice.

### REFERENCES

- Adachi K, Tsubokawa S, Takeuchi T, et al. Strength-[1] ening mechanism of cold drawn wire of in situ Cur Cr composite[J]. J Jap Inst Met, 1997, 61: 397-403.
- [2] Adachi K, Tsubokawa S, Takeuchi T, et al. Plastic deformation of Cr phase in Cur Cr composite during cold rolling[J]. J Jap Inst Met, 1997, 61: 391 - 396.
- Jin Y, Adachi K, Takeuchi T, et al. Microstructural [3] evolution of a heavily cold rolled Cur Cr in situ metal matrix composite[J]. Mater Sci & Eng A, 1996, A212: 149 - 156.
- Jin Y, Adachi K, Takeuchi T, et al. Correlation between the electrical conductivity and aging treatment for a Cur 15wt% Cr alloy composite formed in situ[J]. Materir als Letters, 1997, 32: 307 - 311.
- Jin Y, Adachi K, Takeuchi T, et al. Ageing characteristics of Cur Cr irr situ composite[J]. J Mater Sci, 1998, 33: 1333 - 1341.
- Mihara K, Takeuchi T, Suzuki G H. Effect of Zr on ag-[6] ing characteristic and strength of Cur Cr in situ composites

- [J]. J Jap Inst Met, 1998, 62: 238 245.
- Mihara K, Takeuchi T, Suzuki G H. Effect of Zr on ag-[7] ing characteristics and strength of Cu-Cr in situ composites[A]. Thermec 97. Int Conf Thermomechanical Processing of Steels & Other Materials [C]. TMS, 1997. 1223 - 1229.
- [8] Mihara K, Takeuchi T, Suzuki G H. Effect of Ti on aging characteristics and strength of Cur Cr in situ composites[J]. J Jap Inst Met, 1998, 62: 599 - 606.
- [9] Sakai S, Mihara K, Suzuki G H. The effect of Sn on the properties of Cur Cr im situ composite [A]. Proc 1st Int Conf Advanced Materials Processing [C]. NZ, 2000. 343
- Sun S, Sakai S, Suzuki G H. Effect of the addition of [10] Si on the microstructure and properties of Cur 15Cr irr situ composite materials [A]. Proc 1st Int Conf Advanced Materials Processing [C]. NZ, 2000. 349 - 354.
- [11] Biselli C, Morris D G. Microstructure and strength of CurFe in situ composite after very high drawing strains [J]. Acta Mater, 1996, 44: 493 - 504.

(Edited by PENG Chao qun)